Supporting Information

Selective gas permeation in defect-engineered bilayer graphene

Jiaman Liu[1,2], Lei Jin[2,3], Frances I. Allen[2,4], Yang Gao[2,5], Penghong Ci[2,3], Feiyu Kang[1,6,7]*, Junqiao Wu[2,3]*

[1]Environmental Science and New Energy Technology Engineering Laboratory, Shenzhen Geim Graphene Center (SGGC) and Tsinghua-Berkeley Shenzhen Institute (TBSI), Tsinghua University, Shenzhen 518055, China.
[2]Department of Materials Science and Engineering, University of California, Berkeley, California 94720, United States.
[3]Materials Sciences Division, Lawrence Berkeley National Laboratory, Berkeley, California 94720, United States.
[4]National Center for Electron Microscopy, Molecular Foundry, Lawrence Berkeley National Laboratory, Berkeley, California 94720, USA.
[5]Department of engineering mechanics, Zhejiang University, Hangzhou 310027, China
[6]Institute of Materials Research and Shenzhen Geim Graphene Center (SGGC), Shenzhen International Graduate School (SIGS), Tsinghua University, Shenzhen 518055, China.
[7]Laboratory of Advanced Materials, School of Materials Science and Engineering, Tsinghua University, Beijing 100084, China.
*E-mail: fykang@sz.tsinghua.edu.cn
*E-mail: wuj@berkeley.edu

EXPERIMENT SECTION

Micro-cavity wafer fabrication. Photolithography and reactive ion etching were used to obtain disk-shaped holes with depths of 400-1000 nm in an oxidized silicon wafer with 300 nm silicon oxide on top. The hole diameters were 5 μm. After the holes were fabricated the wafer was cut into chips (around 1 cm×1cm). The chips were then ultrasonically-cleaned in acetone and IPA, for 10 minutes in each case, and finally dried with N_2 gas flow to remove particles and organic contaminants adsorbed on the surface. Prior to graphene exfoliation, oxygen plasma treatment (120 W, 20 sccm H_2, 3 min) was used to further react with remnant hydrocarbons and contaminants adsorbed on the surface and help increase the adhesion between the graphene and the substrate.

Graphene transfer. Immediately after the oxygen plasma treatment, graphite flakes (NGS Naturgraphit GmbH) mechanically-thinned by repeated scotch-tape exfoliation were pressed onto the chip. Additional pressure was gently applied to the tape adhered to the chip using a soft-tipped tweezer. The chip was then heated at 80˚C for ~1 minute on a hot plate to further increase the adhesion. After cooling to room temperature, the tape was slowly peeled off to leave the graphene flakes on the chip. Optical microscopy was used to identify bilayer graphene (BLG) flakes, whereby the underlying SiO_2 layer produced contrast up to 12% to make the graphene visible[1].

He^+ ion irradiation. A He^+ ion microscope (Zeiss Orion NanoFab) equipped with a pattern generator (NPVE from Fibics, Inc.) and operated at 30 keV with probe currents ranging from 0.05 to 0.25 pA (10 μm aperture, spot control 5-6, helium pressure at source 2×10^6 Torr) was used to irradiate the graphene under an angle of incidence of 90˚. For each ion dose, a dwell time of 1 μs and irradiation spot spacing of 0.25 nm was used, which ensures continuity of irradiation over the BLG surfaces (the He^+ beam diameter is ~0.5 nm). As the BLG was suspended over a 5 μm-diameter micro-cavity, the irradiated region was slightly larger (*i.e.* 6 μm in diameter) to cover the entire suspended region.

H_2 plasma treatment. Hydrogen plasma treatment of the graphene was conducted in a plasma-enhanced chemical vapor deposition chamber using the Oxford Plasmalab System 100 (capacitively-coupled type). The plasma treatment was conducted using radio frequency (13.56 MHz), at 350˚C, 1 Torr, and 20 W, for different time periods.

Pressurization chamber. The as-exfoliated graphene samples on the micro-cavity substrate were placed into a home-built pressurized chamber. After repeated inflating (in each test gas) and deflating (in vacuum) for three times, the chamber was re-pressurized with N_2, H_2, He, and CH_4 using charging pressures of ~3000 Torr, ~2000 Torr, ~3000 Torr, and ~3000 Torr, respectively.

AFM measurement. AFM images were obtained in tapping mode using a Veeco Multi-mode AFM.

Raman measurement. Raman spectroscopy was conducted using a Renishaw confocal micro-Raman microscope with a laser excitation wavelength of 488 nm, a 100× objective (NA=0.95) (laser spot size is ~1 μm), and a 2400 g/mm grating. The acquisition time was 10 s and the laser power was set to ~1 mW in order to minimize sample damage.

NOTE S1

According to Ferrari *et al.*[2], in stage 1, *i.e.*, the graphite transforming to nanocrystalline graphite, and the D and D' peak appear and I_D/I_G increases with all peaks broadened. In stage 2, *i.e.*, nanocrystalline graphite transforming to low sp^3 amorphous carbon, the G peak position decreases and I_D/I_G decreases toward 0. In stage 3, *i.e.*, low sp^3 amorphous carbon transforming to high sp^3 (tetrahedrally-coordinated) amorphous carbon, the G peak position increases and I_D/I_G is very low or nearly 0.

NOTE S2

For a clamped circular membrane, the molecular flux, dn/dt, leaking out of the over-pressurized 'blister' can be derived using the ideal gas law and Hencky's solution[3],

$$\frac{dn}{dt} = \frac{\left[\frac{3K(\nu)(Ew\delta^2)}{a^4} \cdot V(\delta) + \pi a^2 C(\nu) P_{atm}\right]}{RT} \frac{d\delta}{dt},$$

where n is the number of moles of gas molecules sealed in the micro-cavity, t is time, E is Young's modulus, ν is Poisson's ratio, w is the thickness, of the membrane, $K(\nu)$ is a coefficient that depends on ν, R is the gas constant, T is temperature, $V(\delta)$ is the total volume of the sealed gas molecules when the membrane is bulged with deflection δ, $V(\delta) = V_0 + V_b(\delta)$, $V_0 = \pi a^2 \cdot h$ is the volume of the disk-shaped micro-cavity, h is the depth of the micro-cavity, $V_b(\delta) = C(\nu)\pi a^2 \delta$, $C(\nu = 0.16) = 0.52$ is a coefficient that depends only on ν, P_{atm} is the atmospheric pressure, a_0 is the diameter of the circular cavity, and a is the diameter of the bulged membrane.

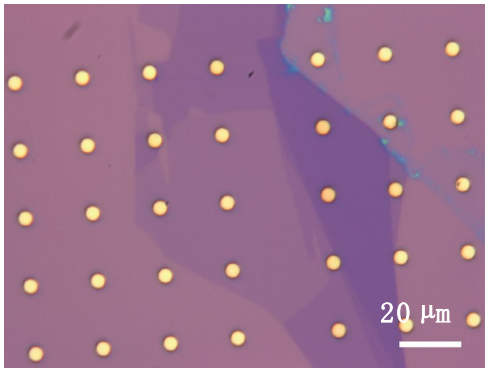

Figure S1. Optical image of BLG exfoliated onto an SiO_2(300nm)/Si wafer with pre-etched holes.

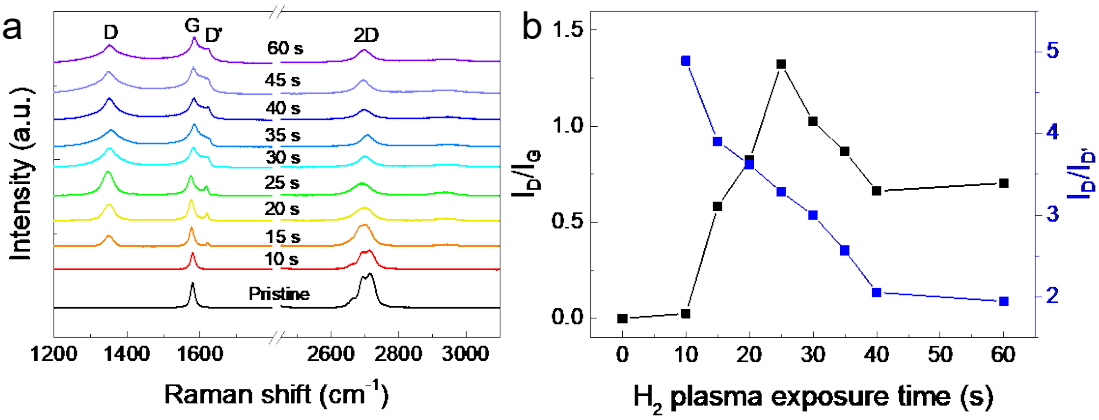

Figure S2. a, Evolution of 2D, D', G, and D Raman peaks as a function of H_2 plasma exposure time. b, Corresponding evolution of I_D/I_G and $I_D/I_{D'}$ versus plasma exposure time.

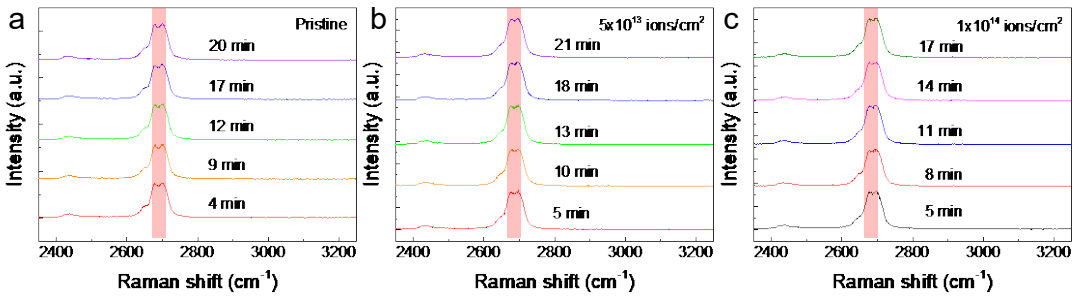

Figure S3. Evolution of Raman spectra for: a, Pristine BLG balloon, b) ion-irradiated BLG balloon using 5×10^{13} ions/cm^2, and c, ion-irradiated BLG balloon using 1×10^{14} ions/cm^2 dose, for different time points upon deflation.

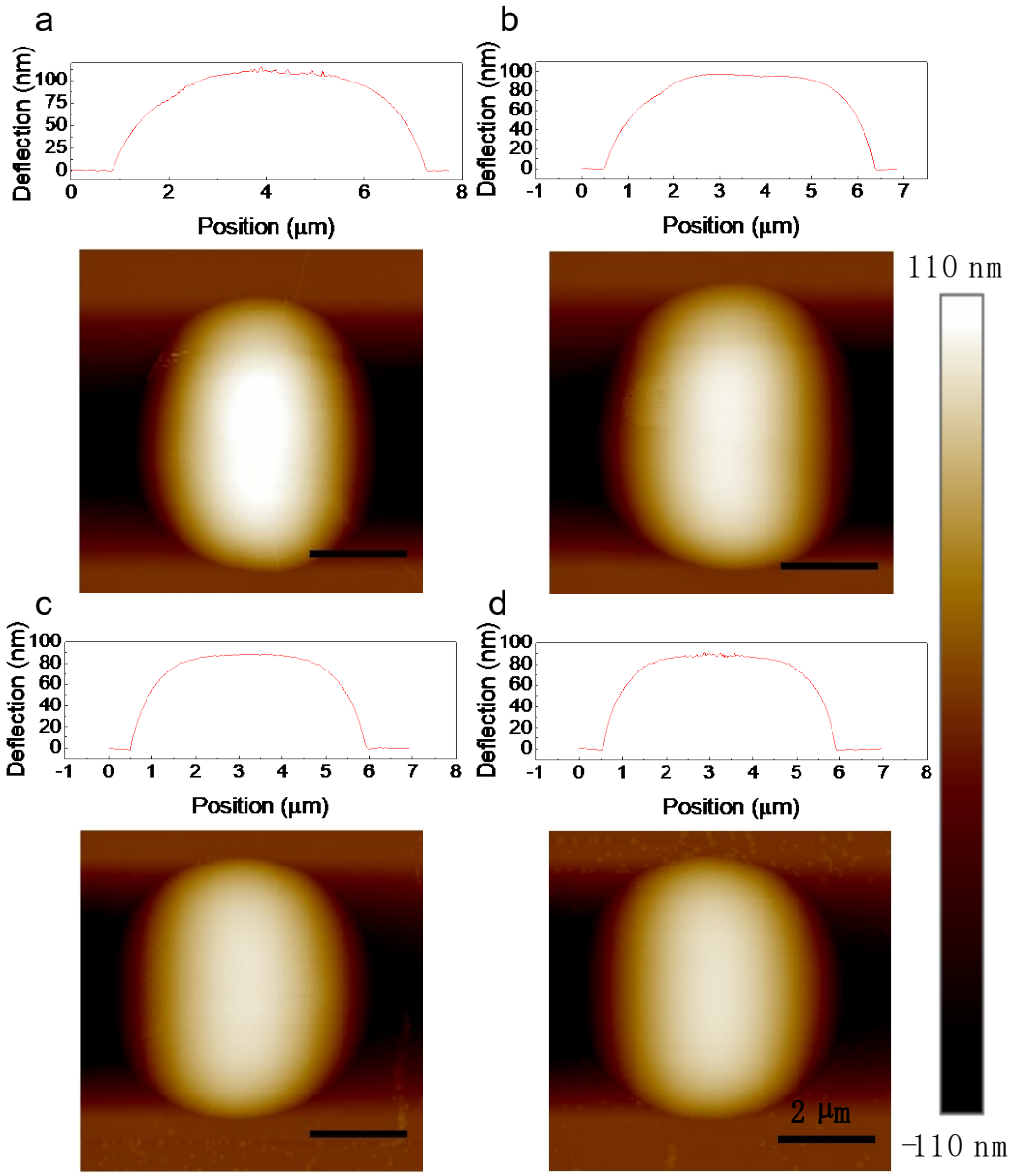

Figure S4. AFM images of a BLG balloon showing different deflections after removal from the pressure chamber: a, 109 nm, b, 96 nm, c, 90 nm, and d, 90 nm.

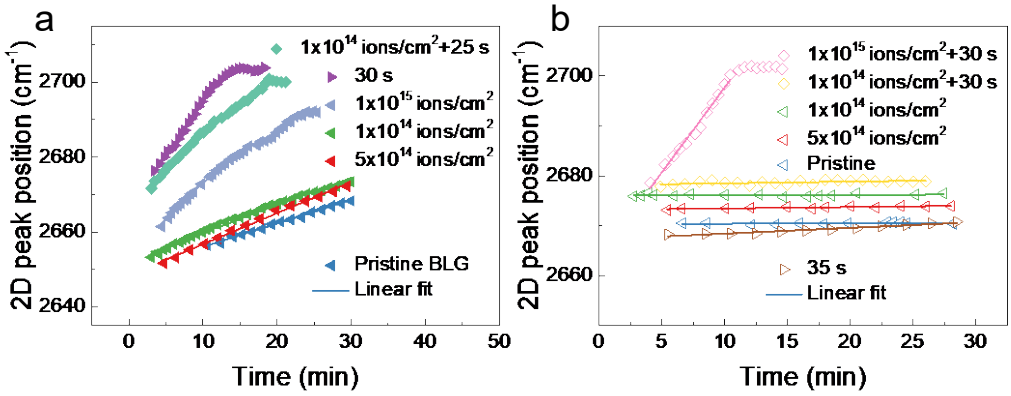

Figure S5. a, He permeance results and b, CH_4 permeance results.

Tabls S1. Experimental values for L_D and n_D calculated from Raman spectra for different irradiation doses.

Irradiation dose (ions/cm^2)	L_D (nm)	n_D (cm^{-2})
5×10^{13}	17.17	1.08×10^{11}
1×10^{14}	13.46	1.76×10^{11}
3×10^{14}	9.20	3.76×10^{11}
5×10^{14}	8.08	4.88×10^{11}
7×10^{14}	7.37	5.86×10^{11}
1×10^{15}	6.92	6.65×10^{11}
2×10^{15}	6.60	7.30×10^{11}
3×10^{15}	6.55	7.43×10^{11}
4×10^{15}	3.15	3.21×10^{12}
5×10^{15}	3.02	3.49×10^{12}

Table S2. N_2 leak rates extracted from the measured Raman peak position shift rates.

Sample	2D peak shift rate (cm^{-1}/min)	Deflection shift rate, $d\delta/dt$ (nm/s)	Maximum deflection, δ (nm)	Radius, a (μm)	Molecular flux, dn/dt (mol/s)	Normalized dn/dt (mol/s·Pa)	Leak rate (mol/s·m^2·Pa)
Pristine BLG	0.0125	0.00056	100	5.8	1.50×10^{-21}	5.01×10^{-27}	4.74×10^{-17}
1×10^{14} ions/cm^2	0.0141	0.00064	100	5.8	1.69×10^{-21}	5.65×10^{-27}	5.35×10^{-17}
5×10^{14} ions/cm^2	0.0129	0.00058	100	5.8	1.55×10^{-21}	5.17×10^{-27}	4.89×10^{-17}
30 s	0.0166	0.00075	100	5.8	1.99×10^{-21}	6.65×10^{-27}	6.29×10^{-17}
35 s	0.1156	0.00521	100	5.8	1.39×10^{-20}	4.63×10^{-26}	4.38×10^{-16}
40 s	9.8100	0.44189	100	5.8	1.18×10^{-18}	3.93×10^{-24}	3.72×10^{-14}
1×10^{14} ions/cm^2 +30 s	0.0534	0.00241	100	5.8	6.40×10^{-21}	2.14×10^{-26}	2.02×10^{-16}
1×10^{15} ions/cm^2 +30 s	7.1028	0.31995	100	5.8	8.51×10^{-19}	2.85×10^{-24}	2.69×10^{-14}
3×10^{14} ions/cm^2 +35 s	30.7308	1.38427	100	5.8	3.68×10^{-18}	1.23×10^{-23}	1.16×10^{-13}

Table S3. H_2 leak rates extracted from the measured Raman peak position shift rates.

Sample	2D peak shift rate (cm^{-1}/min)	Deflection shift rate, $d\delta/dt$ (nm/s)	Maximum deflection, δ (nm)	Radius, a (μm)	Molecular flux, dn/dt (mol/s)	Normalized dn/dt (mol/s·Pa)	Leak rate (mol/s·m^2·Pa)
Pristine BLG	0.04	0.0018	100	5.8	4.79×10^{-21}	2.88×10^{-26}	2.73×10^{-16}
1×10^{14} ions/cm^2	0.09	0.0041	100	5.8	1.08×10^{-20}	6.49×10^{-26}	6.14×10^{-16}
5×10^{14} ions/cm^2	0.15	0.0068	100	5.8	1.80×10^{-20}	1.08×10^{-25}	1.02×10^{-15}
1×10^{15} ions/cm^2	3.68	0.1658	100	5.8	4.41×10^{-19}	2.65×10^{-24}	2.51×10^{-14}
30 s	0.06	0.0027	100	5.8	7.19×10^{-21}	4.33×10^{-26}	4.10×10^{-16}
35 s	7.28	0.3279	100	5.8	8.73×10^{-19}	5.25×10^{-24}	4.97×10^{-14}
1×10^{14} ions/cm^2 +25 s	0.05	0.0023	100	5.8	5.99×10^{-22}	3.60×10^{-26}	3.41×10^{-16}
1×10^{14} ions/cm^2 +30 s	14.67	0.6608	100	5.8	1.76×10^{-18}	1.06×10^{-23}	1.00×10^{-13}
1×10^{15} ions/cm^2 +30 s	14.00	0.6306	100	5.8	1.68×10^{-18}	1.01×10^{-23}	9.56×10^{-14}

Table S4. He leak rates extracted from the measured Raman peak position shift rates.

Sample	2D peak shift rate (cm^{-1}/min)	Deflection shift rate, $d\delta/dt$ (nm/s)	Maximum deflection, δ (nm)	Radius, a (μm)	Molecular flux, dn/dt (mol/s)	Normalized dn/dt (mol/s·Pa)	Leak rate (mol/s·m^2·Pa)
Pristine BLG	0.62	0.0279	100	5.8	7.431×10^{-20}	2.48×10^{-25}	2.35×10^{-15}
1×10^{14} ions/cm^2	0.73	0.0329	100	5.8	8.75×10^{-20}	2.92×10^{-25}	2.77×10^{-15}
3×10^{14} ions/cm^2	0.77	0.0347	100	5.8	9.23×10^{-20}	3.08×10^{-25}	2.92×10^{-15}
5×10^{14} ions/cm^2	0.82	0.0369	100	5.8	9.83×10^{-20}	3.28×10^{-25}	3.11×10^{-15}
7×10^{14} ions/cm^2	0.99	0.0446	100	5.8	1.19×10^{-19}	3.97×10^{-25}	3.75×10^{-15}
1×10^{15} ions/cm^2	1.78	0.0802	100	5.8	2.13×10^{-19}	7.13×10^{-25}	6.75×10^{-15}
30 s	2.71	0.1221	100	5.8	3.25×10^{-19}	1.09×10^{-24}	1.03×10^{-14}
1×10^{14} ions/cm^2 +25s	1.99	0.0896	100	5.8	2.39×10^{-19}	7.97×10^{-25}	7.55×10^{-15}

Table S5. CH_4 leak rates extracted from the measured Raman peak position shift rates.

Sample	2D peak shift rate (cm^{-1}/min)	Deflection shift rate, $d\delta/dt$ (nm/s)	Maximum deflection, δ (nm)	Radius, a (μm)	Molecular flux, dn/dt (mol/s)	Normalized dn/dt (mol/s·Pa)	Leak rate (mol/s·m^2·Pa)
Pristine BLG	0.01	0.0005	100	5.8	1.20×10^{-21}	4.01×10^{-27}	3.79×10^{-17}
1×10^{14} ions/cm^2	0.01	0.0005	100	5.8	1.20×10^{-21}	4.01×10^{-27}	3.79×10^{-17}
5×10^{14} ions/cm^2	0.02	0.0009	100	5.8	2.40×10^{-21}	8.01×10^{-27}	7.58×10^{-17}
35 s	0.12	0.0054	100	5.8	1.44×10^{-20}	4.81×10^{-26}	4.55×10^{-16}
1×10^{14} ions/cm^2 +30 s	0.03	0.0014	100	5.8	3.60×10^{-21}	1.20×10^{-26}	1.14×10^{-16}
1×10^{15} ions/cm^2 +30 s	3.40	0.1532	100	5.8	4.08×10^{-19}	1.36×10^{-24}	1.29×10^{-14}

REFERENCES

(1) Blake, P.; Hill, E. W.; Castro Neto, A. H.; Novoselov, K. S.; Jiang, D.; Yang, R.; Booth, T. J.; Geim, A. K. Making graphene visible. *Appl. Phys. Lett.* **2007,** 91 (6), 063124.

(2) Ferrari, A. C.; Robertson, J. Interpretation of Raman spectra of disordered and amorphous carbon. *Phys. Rev. B* **2000,** 61 (20), 14095.

(3) Koenig, S. P.; Wang, L.; Pellegrino, J.; Bunch, J. S. Selective molecular sieving through porous graphene. *Nat. Nanotechnol.* **2012,** 7 (11), 728-732.